

# Attenuation of Compensatory Right Ventricular Hypertrophy and Heart Failure following Monocrotaline-Induced Pulmonary Vascular Injury by the $\text{Na}^+ - \text{H}^+$ Exchange Inhibitor Cariporide

LING CHEN, XIAOHONG TRACEY GAN, JAMES V. HAIST, QINGPING FENG, XIANGRU LU, SUBRATA CHAKRABARTI, and MORRIS KARMAZYN

Departments of Pharmacology and Toxicology (L.C., X.T.G., J.V.H., M.K.), Medicine (Q.F., X.L.), and Pathology (S.C.), University of Western Ontario, London, Ontario, Canada

Received February 14, 2001; accepted May 1, 2001 This paper is available online at <http://jpet.aspetjournals.org>

## ABSTRACT

Pulmonary hypertension results in compensatory right ventricular (RV) hypertrophy. We studied the role of the  $\text{Na}^+ - \text{H}^+$  exchange (NHE) in the latter process by determining the effect of the NHE-1 inhibitor cariporide after monocrotaline-induced pulmonary artery injury. Sprague-Dawley rats received a control or cariporide diet for 7 days, at which time they were administered either monocrotaline (60 mg/kg) or its vehicle. Twenty-one days later, monocrotaline control, but not cariporide-fed animals, demonstrated increased RV weights and cell size of 65 and 52%, respectively. Monocrotaline alone significantly increased RV systolic pressure and end diastolic pressure by 70 and 94%, respectively, whereas corresponding values with cariporide were significantly reduced to 33 and 42%. Central venous pressure increased by 414% in control animals, which was significantly reduced by cariporide. Monocrotaline treatment produced a decrease in cardiac output of 28 and 8% in the absence or presence of

cariporide ( $P < 0.05$  between groups), respectively. Although body weights were significantly lower in both monocrotaline-treated groups compared with vehicle treatment, with cariporide the net gain in body weight was twice that seen in the monocrotaline-treated animals without cariporide. Monocrotaline also increased RV NHE-1 and atrial natriuretic peptide mRNA expression, which was abrogated by cariporide. Monocrotaline-induced myocardial necrosis, fibrosis, and mononuclear infiltration was completely prevented by cariporide. Cariporide had no effect on monocrotaline-induced pulmonary intimal wall thickening. Our results demonstrate that cariporide directly attenuates myocardial dysfunction after monocrotaline administration independent of pulmonary vascular effects. NHE-1 inhibition may represent an effective adjunctive therapy that selectively targets myocardial hypertrophic responses in pulmonary vascular injury.

Pulmonary hypertension represents an important clinical problem that can result in development of right ventricular (RV) hypertrophy and heart failure (Krowka, 2000; Gaine and Rubin, 1998) and which is associated with a high rate of mortality (Lilienfeld and Rubin, 2000). The ventricular hypertrophic response is probably mediated to a large degree by the production of paracrine and autocrine hypertrophic agents linked to signal transduction-dependent regulation of transcriptional factors. Recent studies suggest that left ventricular myocardial hypertrophy following infarction is dependent at least in part on the activity of the sodium-hydrogen exchange (NHE), an electroneutral antiporter representing the primary pathway for proton extrusion in the cardiac cell in exchange for sodium ion

influx (reviewed in Karmazyn et al., 1999; Cingolani, 1999). Accordingly, inhibiting the primary NHE isoform found in the myocardium (NHE-1) reduces both the hypertrophic as well as heart failure responses after infarction in rats (Yoshida and Karmazyn, 2000; Kusumoto et al., 2001). Further supporting the concept of NHE-1 involvement are studies demonstrating reduced hypertrophy in cultured cells exposed to various hypertrophic factors when treated with NHE inhibitors (Hori et al., 1990; Yamazaki et al., 1998).

Although emerging evidence supports NHE involvement in postinfarction left ventricular failure, nothing is known about the role of the antiporter in right ventricular hypertrophy secondary to pulmonary hypertension. Among the most widely studied animal models of right ventricular hypertrophy and right heart failure is the administration of the pyrrolizidine alkaloid monocrotaline (MCT), which produces a relatively rapid (within a few weeks) pulmonary hyperten-

This study was funded by a grant from the Canadian Institutes of Health Research. Dr. Karmazyn is a Career Investigator of the Heart and Stroke Foundation of Ontario.

**ABBREVIATIONS:** RV, right ventricle; ANP, atrial natriuretic peptide; MCT, monocrotaline; NHE-1,  $\text{Na}^+ - \text{H}^+$  exchange isoform 1; LV, left ventricle; RT-PCR, reverse transcriptase-polymerase chain reaction; dNTP, deoxynucleotide triphosphate; GAPDH, glyceraldehyde-3-phosphate dehydrogenase; PKC, protein kinase C; DEPC, diethyl pyrocarbonate.

sion resulting in compensatory right ventricular hypertrophy and heart failure (Rosenberg and Rabinovitch, 1998; Schultze and Roth, 1998; Nakazawa et al., 1999; Pichardo et al., 1999). This experimental approach is advantageous in the sense that the myocardial involvement occurs secondarily to initiating factors that are of noncardiac origin, thus allowing the possibility of closer mechanistic assessment of therapeutic strategies. Moreover, as NHE inhibitors are also protective agents in the ischemic myocardium, this approach also permits the assessment of the effect of NHE-1 inhibition on myocardial hypertrophy and heart failure independent of infarct size reduction. We therefore hypothesized that NHE-1 inhibition could attenuate the right ventricular hypertrophic response after MCT administration. Accordingly, we examined the effect of the NHE-1-specific inhibitor cariporide on the myocardial responses 3 weeks after MCT administration to rats.

## Materials and Methods

**Experimental Protocol.** One hundred and eight virus-free male Sprague-Dawley rats weighing 200 to 250 g were maintained in the Health Sciences Animal Care facilities of the University of Western Ontario in accordance with the guidelines of the Canadian Council on Animal Care (Ottawa, ON, Canada). The animals were randomly assigned to either the control chow or an identical diet containing 3000 parts per million of cariporide (Aventis Pharma, Frankfurt, Germany), which resulted in mean plasma levels of the drug of  $381 \pm 29$  ng/ml ( $n = 10$ ). After 1 week of feeding, the animals were randomized to receive subcutaneously administered MCT (60 mg/kg b.wt., Sigma-Aldrich Canada Ltd, Oakville, ON, Canada) or equal volumes of vehicle. MCT was prepared by dissolving it in 1 N HCl. The pH was neutralized with 0.5 N NaOH, and the volume of the solution was adjusted with phosphate-buffered saline (pH 7.40) to achieve a concentration of 30 mg/ml. Animals were subsequently maintained for a further 21 days on their respective diets, at which time experimental data were collected as described below. In addition, plasma was collected from 10 cariporide-treated rats (5 sham, 5 MCT-treated) for determination of plasma drug concentrations.

**Hemodynamic Measurements.** The animals were weighed and then anesthetized with sodium pentobarbital sodium (50 mg/kg b.wt., i.p.) and buprenorphine (0.03 mg/kg b.wt., s.c.). Animals were then intubated and ventilated (tidal volume, 10 ml/kg; ventilator rate, 70 breaths/min) with air using a rodent respirator (model 683, Harvard Apparatus, Holliston, MA). A standard lead II electrocardiogram was obtained using a Grass model 7P6 recorder (Astro-Med, West Warwick, RI), and a thermistor probe was inserted into the rectum to measure core temperature, which was maintained at 37–38°C with the aid of a heating pad. Arterial pressure and left ventricular pressure were sequentially measured with a PE-50 Intra-medical polyethylene tube (0.023-inch i.d. and 0.038-inch o.d., Clay Adams, Parsippany, NJ) introduced into the right carotid artery by the neck cut-down and then advanced to the ascending aorta and the left ventricles, respectively. Central venous pressure and right ventricular pressure were sequentially measured with a PE-50 polyethylene tube that was slightly modified by heating and introduced into the right external jugular vein and advanced to the right atrium and the right ventricle, respectively. The catheters were connected to a pressure transducer (Model PX-1800, Baxter Healthcare Co., Irvine, CA) positioned at the mid-thorax of the animal. The transducers were connected to a BioPac Computer Data Acquisition System (Harvard Apparatus). The position of the catheter was confirmed by the waveform of the pressure tracing from the computer screen using AcqKnowledge software (version 3.2, Harvard Apparatus). After the catheterization procedures, a 10-min stabilization was allowed be-

fore the measurements were recorded and stored in the computer at a sampling rate of 100 Hz.

To assess cardiac output, the chest was opened by the middle sternal incision. The thymus and heart were exposed, and the right pleura was maintained intact. The thymus was then divided into the left and right lobe to expose the aorta, and the ascending aorta was gently separated from the pulmonary artery. A Transonic flowprobe connected to a T206 Transonic flowmeter (Transonic Systems Inc., Ithaca, NY) was placed around the ascending aorta. A chest tube was placed percutaneously, and the thoracotomy was closed in layers. The chest was then evacuated to allow inflation of the lung. A 10-min stabilization following surgery was allowed before the digital readings of cardiac output over a 1-min period were recorded.

The animals were sacrificed at the end of the hemodynamic measurement by an overdose of pentobarbital administered intravenously via the right ventricular catheter. The heart and lungs were removed en bloc for further analysis (see below).

**Determination of Heart Weights.** The heart was removed, the chambers were opened, and any excess blood was dried with paper towels, after which the heart was weighed. The atria and large blood vessels were then removed. The hearts were separated into the right ventricle free wall (RV) and the left ventricle (LV) including the septum and weighed separately.

**Histology.** Myocardial tissues (LV and RV,  $n = 10$ ) were fixed by immersion in 10% buffered formalin and embedded in paraffin for morphological analyses. Five-micrometer sections stained with hematoxylin and eosin as well as Gomori's trichrome stain were used for morphological analyses. The samples were coded and the slides were subjected to light microscopic examination by one of the authors (S.C.), who was unaware of the specimen identity or treatment group.

**NHE-1 and ANP mRNA Expression.** Total RNA was isolated from either right or left ventricles and washed with 500  $\mu$ l of ethanol (75% v/v) in diethyl pyrocarbonate (DEPC) water. The tubes were recentrifuged at 12,000g for 5 min, and the ethanol was decanted. All the RNA pellets were air-dried and redissolved in 50 to 100  $\mu$ l of DEPC water. The RNA concentration was measured spectrophotometrically using an RNA/DNA calculator at 260 nm (Genequant II, Amersham Pharmacia Biotech Ltd., Cambridge, UK).

We determined NHE-1 expression using competitive reverse transcriptase polymerase chain reaction. Competitors were created using commercial DNA construction kits (Takara Shuzo, Otsu, Japan) such that the sequences at both ends of the competitor were complementary to the same primers for amplifying the target DNA and the sizes of the competitor DNA fragments were comparable with the target DNA fragments, assuring the same dynamics of the amplification reaction for the target and the competitor DNA fragments. Optimal competitor concentrations for each target gene were established by viewing the electrophoresis band pattern with serial dilutions of the competitor. The amplification was carried out using the NHE-1, primer 1 [(+), 5'-TCTGTGGACCTGGTGAATGA-3'] and primer 2 [(-), 5'-GTCACTGAGGCAGGGTTGTA-3'] with a predicted product size of 210 bp and a competitor size of 292 bp. Reactions were performed in 25- $\mu$ l volumes containing 2.5  $\mu$ l of 10 $\times$  PCR-buffer, 1  $\mu$ l of 50 mM MgCl<sub>2</sub>, 1.25  $\mu$ l of deoxynucleotide triphosphate (dNTP) mix, 1.25  $\mu$ l of each amplification primer, 0.25  $\mu$ l of Platinum *Taq* polymerase, 1  $\mu$ l of the RT product and 1  $\mu$ l of the competitor in optimal concentration. The initial cycle was carried out using 3 min at 94°C for denaturation, 1 min at 54°C for annealing, and 3 min at 72°C for extension. Subsequent cycles of PCR were performed using the following conditions: denaturation, 45 s at 94°C; annealing, 45 s at 54°C; extension, 1 min at 72°C; and final extension, 7 min at 72°C. The linearity of the PCR reaction was established by analyzing the PCR product with variable amounts of template and competitor and variable cycle numbers. In our study, we used 30 cycles of amplification for NHE-1.

Semiquantitative determination of ANP mRNA was assessed by RT-PCR. For reverse transcription of mRNA, 3  $\mu$ g of total RNA from

each sample were used. Oligo(dT) (0.5  $\mu$ g) and DEPC water was added to each PCR tube to a final volume of 12  $\mu$ l. The tubes were subsequently heated at 70°C for 10 min exposing the poly(A) tails characteristic of mRNA to the oligo(dT), thereby priming the mRNA for reverse transcription. Next, dNTPs (0.5 mM), dithiothreitol (0.5 mM), Moloney murine leukemia virus reverse transcriptase (100 units, Invitrogen, Burlington, ON, Canada), and first strand buffer (1 $\times$ , Invitrogen) were added to a final volume of 20  $\mu$ l to each PCR tube. Finally, the RNA was reverse transcribed into cDNA by reverse transcriptase at 37°C for 1 h.

Two microliters of cDNA from each sample was placed into PCR reaction tubes (0.2-ml ultrathin wall). Subsequently, PCR buffer (1 $\times$ , Invitrogen), dNTPs (200  $\mu$ M), MgCl<sub>2</sub> (1.5 mM), predesigned forward and reverse primers (1.5  $\mu$ mol), *Taq* polymerase (0.5 units, Invitrogen), and sterile H<sub>2</sub>O to a final volume of 25  $\mu$ l were added to each PCR reaction tube. The forward and reverse primers for rat ANP were 5'-CTGCTAGACCACCTGGAGGA-3' and 5'-AAGCTGTTCAGCCTAGTCC-3', respectively. The forward and reverse primers for glyceraldehyde phosphate dehydrogenase were 5'-AAAGGGCATCCTGGGC-TACA-3' and 5'-CAGTGTGGGGCTGAGTTG-3', respectively. The PCR tubes were then placed in the thermal cycler, and a heat-cycling program was executed. The melting temperature for the cDNA was set at 94°C, and the *Taq* polymerase activation temperature was set at 72°C. Annealing temperature for ANP and GAPDH was 60 and 66°C, respectively. Equal aliquots of cDNA were submitted to a subsaturation number of PCR cycles (40 and 20 cycles for ANP and GAPDH, respectively) as determined by the sequential cycling experiments.

Amplification of cDNA for ANP and GAPDH was carried out independently. PCR products of ANP and GAPDH were 320 bp and 297 bp, respectively. Samples were then electrophoresed in 1.5% agarose gels containing ethidium bromide and quantified via computer densitometry.

**Myocyte Isolation and Measurements.** Ten hearts per group were collected for myocyte isolation, and measurements were made using methods from this laboratory described previously (Hoque et al., 2000). In brief, hearts were removed and perfused immediately with Ca<sup>2+</sup>-free HEPES-buffered solution for 3 min followed by 10 min of perfusion with one containing 1.66 mg/ml collagenase type II (Worthington Biochemical Corp, Lakewood, NJ) and 0.1 mg/ml protease type XIV (Sigma-Aldrich Canada Ltd). The collagenase was then washed out with a solution containing 0.2 mM CaCl<sub>2</sub>. The heart was removed and then separated into the RV free wall and LV. The left and right ventricular tissues were separately chopped with scissors and incubated in buffer with 0.2 mM CaCl<sub>2</sub> at 37°C for 15 min, filtered, and centrifuged for 45 s. A cell aliquot was transferred to a stage of an inverted microscope (Leica Microsystem, Wetzlar GmbH, Germany) equipped with a digital camera (model PDMC-2, Polaroid Canada, Etobicoke, ON, Canada). The 10 images per sample were photographed using DirectPhoto software (v2.0, Polaroid Canada) at a 200 $\times$  magnification and stored in a computer (Dell XPS T500). The cell area of 10 cells per image was measured using Mocha software (version 1.2, SPSS Science, Chicago, IL). An average was calculated for each of the 50 cells analyzed for each sample.

**Measurement of Pulmonary Artery Wall Thickness.** The lungs were collected immediately after the animals were sacrificed. Blood was washed out by 0.9% saline, and lungs were gently dried with paper towels. The samples were then submerged in 10% buffered formalin for at least 48 h before which the right lower lobe was embedded in paraffin. Elastin stains were performed on sections 5  $\mu$ m thick. The degree of pulmonary vascular remodeling was assessed by measuring the percentage of wall thickness of terminal small arteries (vessels indexed to respiratory bronchioles). At least 10 horizontally cut terminal small arteries were photographed using a Leica inverted microscope equipped with a Polaroid digital camera as described for myocytes. The images were stored on the hard drive of a Dell computer system and analyzed using Mocha software (SPSS Science). Orthogonal intercept measurement modified from method described previously (Gundersen et al., 1978; Jensen et al., 1979) was used to generate 10 random measurements of medial wall thickness (the distance between the internal and external lamina) and 10 random measurements of diameter of the vessels (distance between the external lamina). Harmonic means were taken for each vessel, and an average was calculated for each of the 10 vessels analyzed for each sample. Percentage of wall thickness was expressed as the medial wall thickness divided by the diameter of the vessel  $\times$  100.

**Statistical Analysis.** Analyses were performed using SigmaStat (SPSS Science). The variables between groups were compared by analysis of variance and subsequent multiple comparisons by the Student-Newman-Keuls test. A value of  $P < 0.05$  was considered statistically significant. All values were expressed as mean  $\pm$  S.E.M.

## Results

As shown in Table 1, animals treated with MCT exhibited significantly depressed body weight gains over the 3-week follow-up period. However, although body weight gain was still significantly lower from control, MCT-treated animals treated with cariporide demonstrated a 2-fold higher increase in body weight over the 3-week period compared with untreated animals. Neither heart rates nor mean arterial pressures were affected by any treatment.

**RV Tissue Weights and Cell Size.** These results are summarized in Fig. 1 and demonstrate significant increases in RV weight and cell area following MCT treatment without cariporide with no direct effect of cariporide itself in the absence of MCT. The relative increases in RV weight and cell size were 65 and 52%, respectively, in rats that did not receive cariporide. The change in cell area in the presence of cariporide was 21%. RV weight was actually 12% less in hearts from the MCT-cariporide group, although neither tissue weight nor cell size were significantly changed. There were no significant changes in either LV weight or LV myocyte size with any treatment (data not shown).

TABLE 1

General animal characteristics and cardiovascular parameters in control and MCT-treated animals

Values represent means  $\pm$  S.E.M.

Parameter	Untreated		Cariporide	
	Control (n = 18)	MCT (n = 20)	Control (n = 18)	MCT (n = 22)
Baseline BW (g)	273 $\pm$ 7.6	262 $\pm$ 3.1	272 $\pm$ 3.1	267 $\pm$ 3.6
$\Delta$ BW (g)	153 $\pm$ 5.7	25 $\pm$ 6.5***	147 $\pm$ 5.5	50 $\pm$ 4.2***†
HR (beats/min)	363 $\pm$ 11	386 $\pm$ 13	352 $\pm$ 15	376 $\pm$ 11
MAP (mm Hg)	113 $\pm$ 4.6	78 $\pm$ 6***	111 $\pm$ 4.5	91 $\pm$ 5**
LVSP (mm Hg)	132 $\pm$ 3.3	98 $\pm$ 4.6***	135 $\pm$ 3.4	107 $\pm$ 4.3***

Baseline BW, body weights immediately prior to MCT administration;  $\Delta$  BW, increase in body weight over the 3-week follow-up period. All other values were obtained 3 weeks after MCT administration. HR, heart rate; LVSP, left ventricular systolic pressure; MAP, mean arterial pressure.

\*\*  $P < 0.01$ , \*\*\*  $P < 0.001$  from respective control value; †  $P < 0.05$  from MCT untreated group.

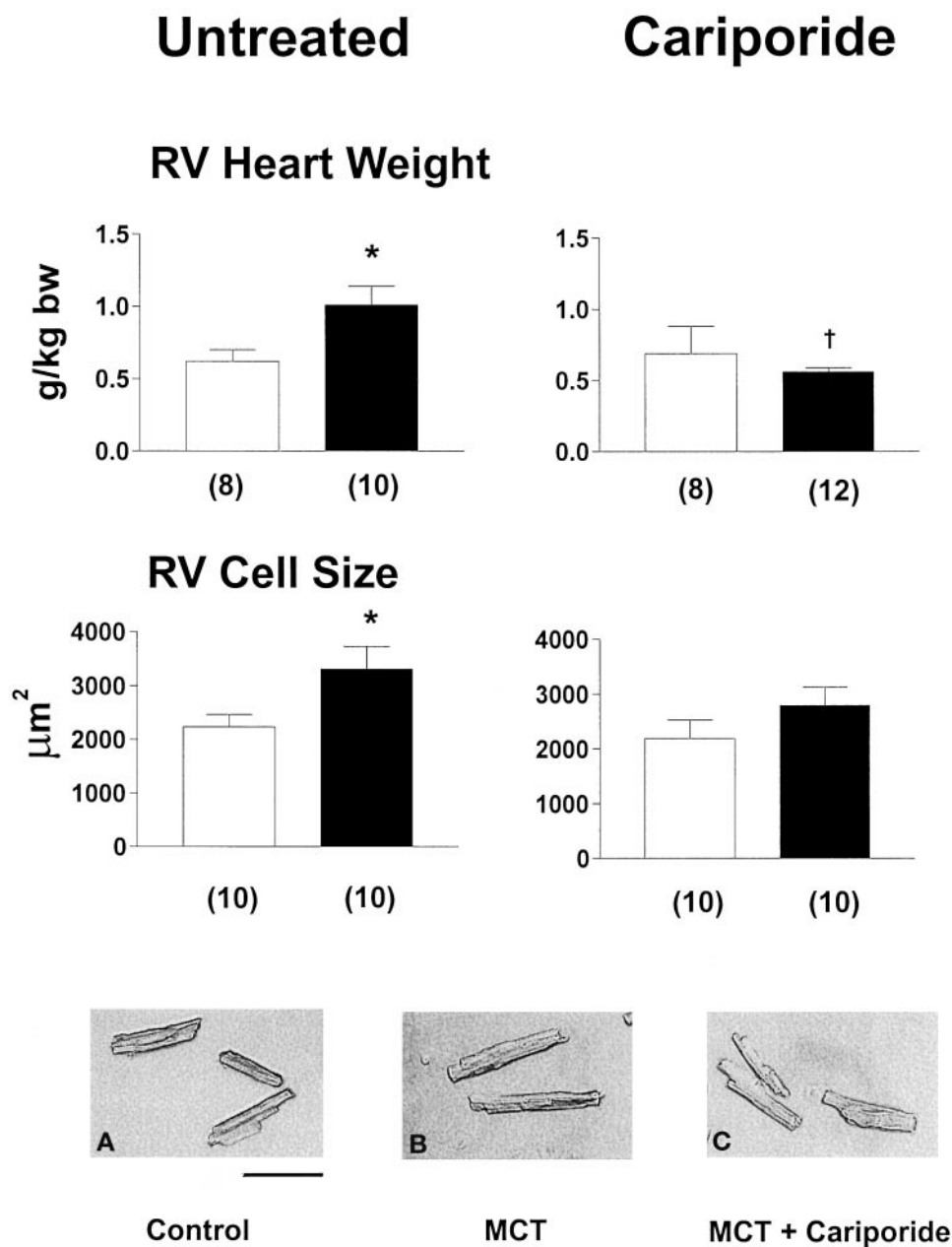


**Fig. 1.** Indices of RV hypertrophy in terms of heart weight or cell size 3 weeks after MCT administration (closed columns). Open columns indicate control (sham) treatments. Values are means  $\pm$  S.E.M. \* $P < 0.05$  from respective control group; † $P < 0.05$  from respective MCT untreated group. Numbers in parentheses indicate number of samples studied; however, for cell measurements 50 cells were analyzed and averaged to obtain one value. Photographs at bottom show examples of RV myocytes from sham untreated animals (A), MCT untreated animals (B), and MCT cariporide animals (C). Scale bar, 100  $\mu$ m. bw, body weight.

**RV Hemodynamic Responses.** To further determine the degree of RV responses to MCT treatment, we measured intraventricular pressures as summarized in Fig. 2. RV systolic pressures were significantly elevated by 70% in MCT-treated rats, although the degree of elevation was significantly attenuated by cariporide to 33%. Moreover, as shown in Fig. 2, the relative elevation in RV end diastolic pressures was similarly markedly attenuated in cariporide-treated animals. Thus, RV end diastolic pressure increased by 94% ( $P < 0.001$ ) in MCT-treated animals without cariporide, whereas with cariporide this elevation was attenuated to 42% ( $P < 0.05$ ).

**RV ANP and NHE-1 mRNA Expression.** MCT treatment was associated with increased RV expression of ANP as well as NHE-1 mRNA. Compared with tissues of sham (neither MCT or cariporide) animals, NHE-1 mRNA increased 2-fold with MCT treatment ( $P < 0.05$ ), although this was completely abrogated by cariporide (Fig. 3). MCT treatment

also resulted in a 4-fold elevation in ANP expression; however, this was prevented by cariporide (Fig. 3). There were no changes in either NHE-1 or ANP LV expression with any treatment (not shown).

**Heart Failure.** A major hallmark associated with MCT-induced RV responses is the development of heart failure. To document and characterize more precisely the degree of heart failure, both cardiac output and central venous pressures were determined. The degree of heart failure was profound, as evidenced by a 28% reduction in cardiac output in MCT-treated rats without cariporide ( $P < 0.001$ ), whereas in the presence of the NHE-1 inhibitor the reduction in cardiac output was significantly attenuated to 8%, although the degree of reduction was significant (Fig. 4).

As shown in Fig. 5, hemodynamic dysfunction in MCT-treated animals was associated with a marked increase in central venous pressure irrespective of cariporide treatment ( $P < 0.001$  for both groups), although as with cardiac output,

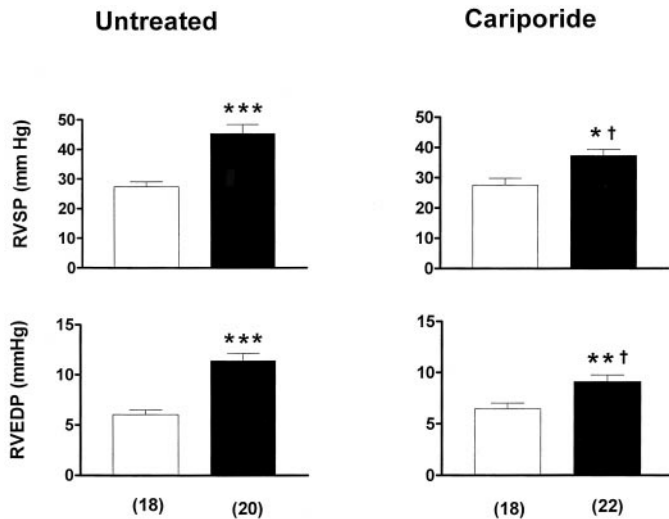


**Fig. 2.** Right ventricular systolic (RVSP) and end diastolic (RVEDP) pressures in rats 3 weeks after MCT (■) or vehicle (control, □) administration. Values are means  $\pm$  S.E.M. \*\*\* $P$  < 0.01, \*\*\*\* $P$  < 0.001 from respective control group; † $P$  < 0.05 from respective MCT untreated group. Numbers in parentheses indicate number of samples studied.

the elevation in venous pressure was significantly less (414 versus 294%,  $P$  < 0.05) with cariporide.

**Myocardial Morphology.** In terms of myocardial tissues, no abnormalities were observed in hearts of animals not treated with MCT. However, 8 of 10 RV samples from MCT-treated animals showed the presence of focal myocyte necrosis and mononuclear leukocyte infiltration as well as early fibrosis. We observed no histological abnormalities in MCT-treated animals given cariporide. Representative micrographs are shown in Fig. 6. No LV changes were observed in any group (not shown).

**Pulmonary Vascular Morphology.** Because the primary cause of MCT-induced myocardial complications reflects initial effects of this agent on pulmonary vessel remodeling, we determined whether the salutary effects of cariporide reflected an effect on the initial pulmonary response of MCT or whether cariporide's effect was attributable to cardiospecific influences. As noted under *Discussion*,

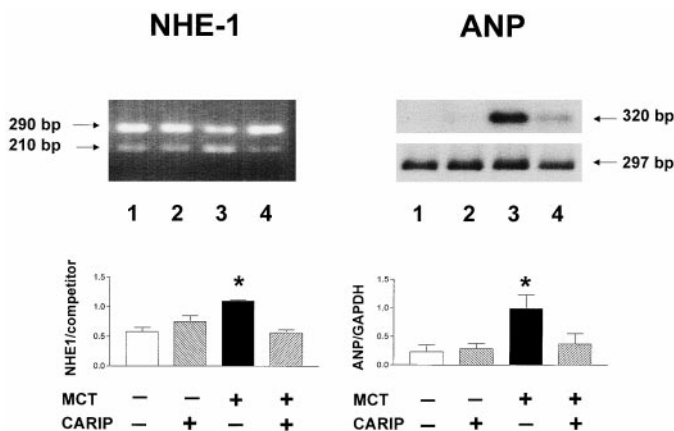


**Fig. 3.** RT-PCR analysis of NHE-1 and ANP expression in RV after various treatments. Top panels, examples of ethidium bromide-stained gels of RT-PCR products according to the following treatments: 1) untreated; 2) cariporide (CARIP) only; 3) MCT only; 4) MCT plus cariporide. Data were quantified using densitometry and are presented as ratio to competitor for NHE-1 or GAPDH as the reference gene for ANP. Values are means  $\pm$  S.E.M. \* $P$  < 0.05 from control group.

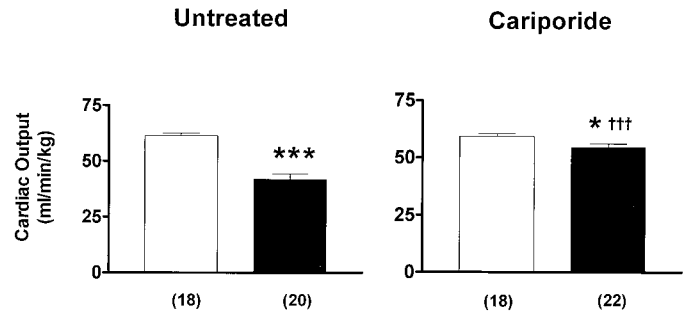


**Fig. 4.** Cardiac output in rats 3 weeks after MCT (■) or vehicle (control, □) administration. Values are means  $\pm$  S.E.M. \* $P$  < 0.05, \*\*\*\* $P$  < 0.001 from respective control group; ††† $P$  < 0.001 from respective MCT untreated group. Numbers in parentheses indicate number of samples studied.

this is of further interest as there is evidence that NHE may be involved in vascular remodeling responses to various factors. As summarized in Fig. 7, MCT produced a significant (39%) increase in wall thickening. However, in contrast to the inhibitory effects of cariporide on cardiac responses, the degree of medial wall thickness was virtually identical (41%) to that seen without cariporide.

## Discussion

It is well established that NHE-1 inhibition protects the acutely ischemic and reperfused myocardium (Pierce and Czubyrt, 1995; Karmazyn et al., 1999); indeed, this approach appears to be the most effective cardioprotective strategy today (Gumina et al., 1999; Gumina and Gross, 1999). Emerging evidence suggests that this antiporter may also be important in tissue hypertrophy in response to a variety of stimuli. Accordingly, the primary goal of this study was to evaluate the potential contribution of the NHE to compensatory myocardial hypertrophic and subsequent responses that occur after pulmonary hypertension. The hypothesis that NHE may be involved in these processes stems from both in vitro and in vivo studies which have shown that NHE inhibition results in diminished hypertrophy in cardiac myocytes in response to hypertrophic factors or following left coronary artery ligation (Hori et al., 1990; Yamazaki et al., 1998; Cingolani, 1999; Karmazyn et al., 1999; Yoshida and Karmazyn, 2000; Kusumoto et al., 2001). NHE may also be involved in vascular hypertrophy. For example, neointimal thickening following arterial injury in rats has been shown to be attenuated by NHE inhibitors (Kranzhöfer et al., 1993). Moreover, cariporide has recently been shown to reduce mesenteric artery remodeling and hypertrophy in the diabetic rat (Jandeleit-Dahm et al., 2000). Thus, taken together, NHE inhibition could represent an effective approach toward minimizing hypertrophic pathological processes. Our results are the first to demonstrate that NHE-1 inhibition reduces myocardial responses to pulmonary artery injury. They further suggest that these effects occur independent of any influence on the primary pulmonary artery responses.

We used the MCT model of pulmonary hypertension because this approach has been well characterized and resembles clinical pulmonary vascular disease (Rosenberg and Rabinovitch, 1998; Schultze and Roth, 1998; Nakazawa et al., 1999). MCT produces its effects primarily by injuring pulmonary vessel endothelium, resulting in reduced vasodilating

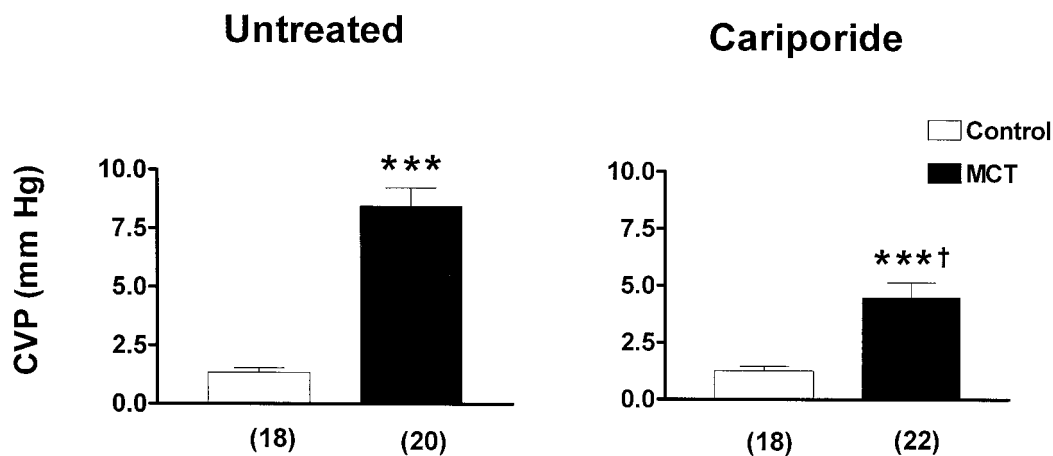


**Fig. 5.** Central venous pressure (CVP) in rats 3 weeks after MCT or vehicle (control) administration. Values are means  $\pm$  S.E.M. \*\*\* $P$  < 0.001 from respective control group; † $P$  < 0.05 from respective MCT untreated group. Numbers in parentheses indicate number of samples studied.

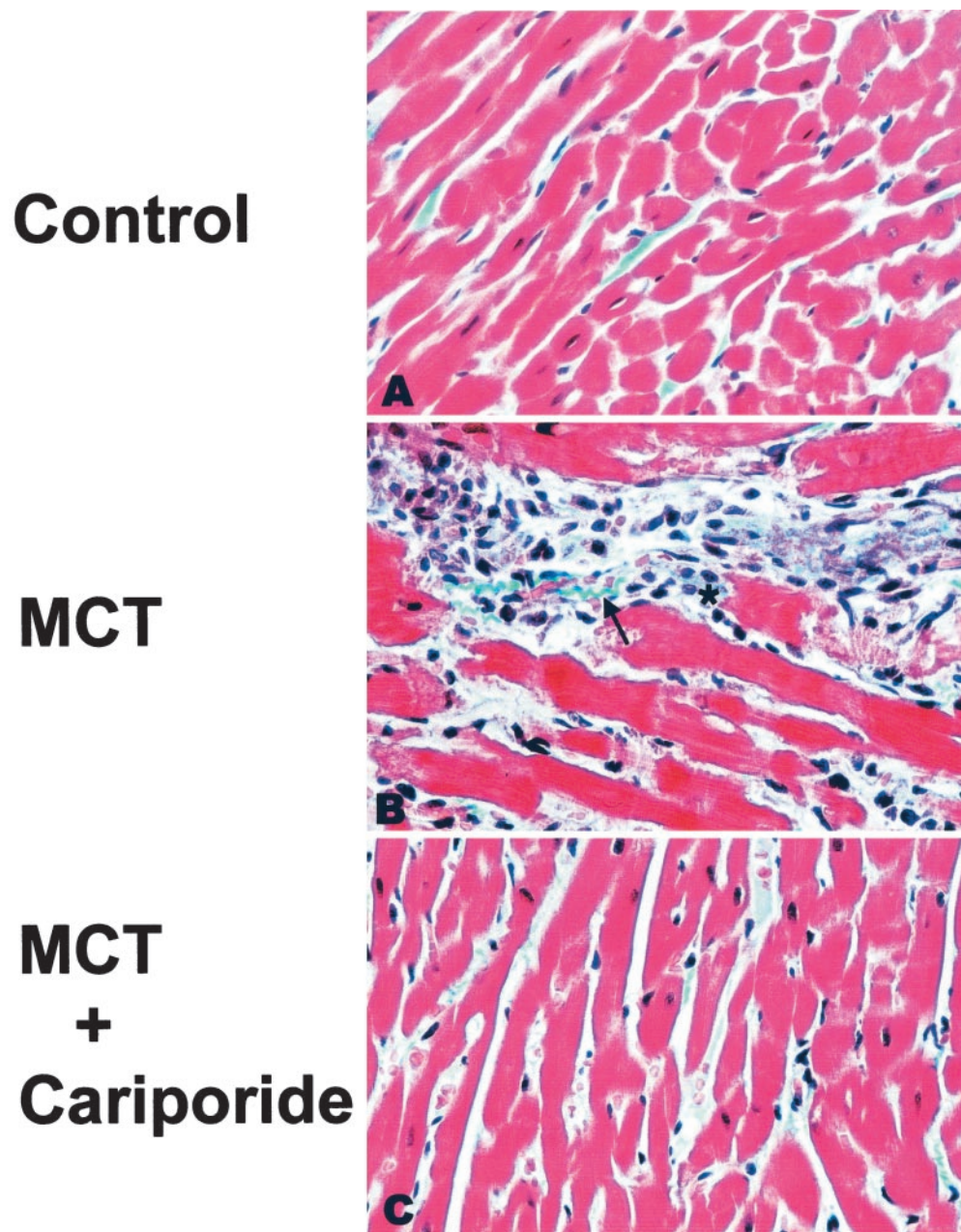


**Fig. 6.** Representative photomicrographs from the right ventricular myocardium of untreated control rat (A), MCT-treated rat (B), and MCT-treated rat provided cariporide (C). B, examples of mononuclear infiltrations and myocyte damage (asterisk) as well as early fibrosis (arrow). Trichrome stain: original magnification, 400 $\times$ .

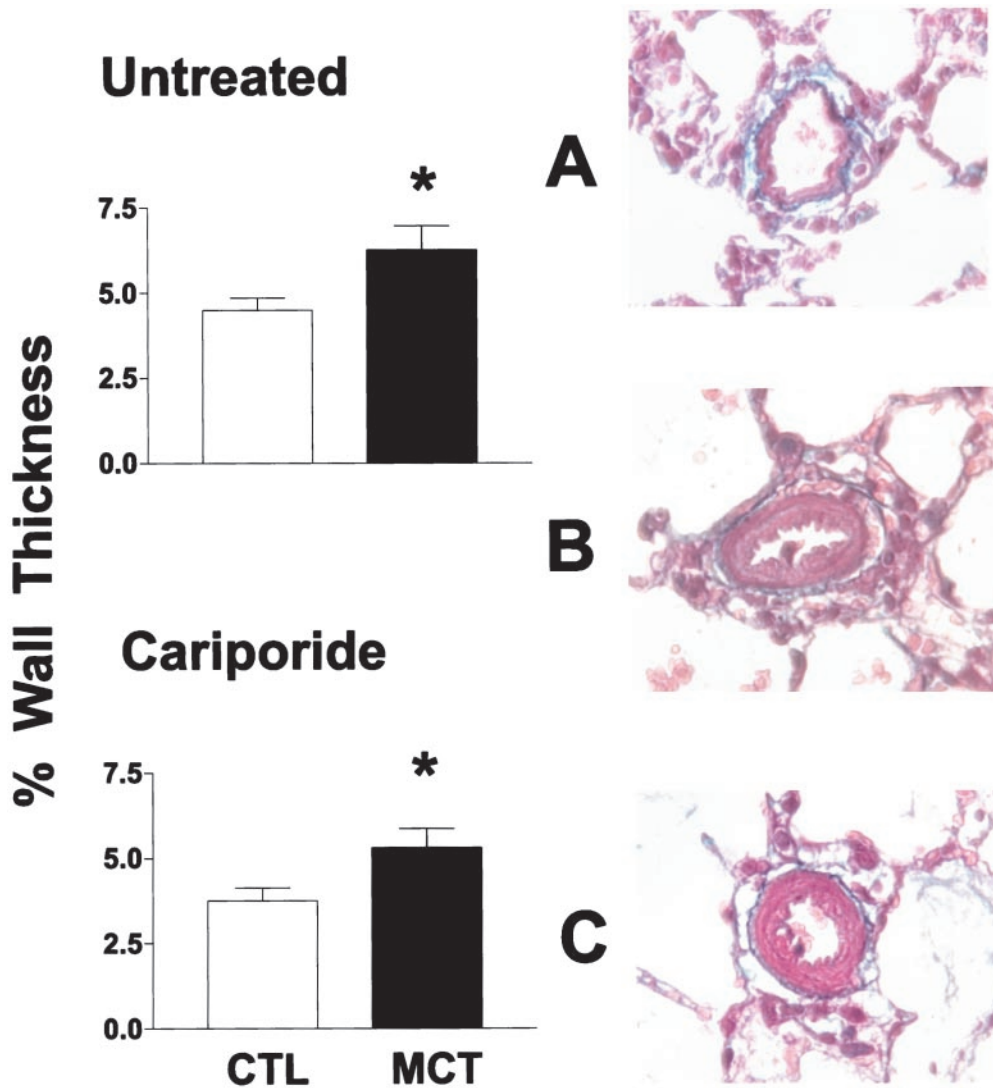


**Fig. 7.** Left panel, pulmonary artery wall thickness in rats 3 weeks after MCT or vehicle control (CTL) administration. Values are means  $\pm$  S.E.M. \* $P < 0.05$  from respective sham group. Percentage of wall thickness was calculated as described under *Materials and Methods*. Right panel, representative micrographs of pulmonary artery vessels after vehicle (A) or MCT administration without (B) or with (C) cariporide treatment. Elastin stain: original magnification, 400 $\times$ .

responses and increased vascular resistance (Schultze and Roth, 1998). Blocking the pulmonary hypertension represents a key therapeutic approach for the deleterious effects of MCT in rats and clearly is of importance in developing effective strategies for this life-threatening condition.

As noted above, we hypothesized that provision of a NHE-1-specific inhibitor should diminish both the vascular and myocardial responses to MCT since NHE-1 is the primary NHE isoform in both myocardium as well as vascular smooth muscle cells. However, our findings demonstrate that pulmonary artery remodeling as determined by vessel thickness after MCT treatment was unaffected by cariporide. In view of the studies referred to above suggesting that NHE-1 may also be important in vascular remodeling (Kranzhöfer et al., 1993; Jandeleit-Dahm et al., 2000), we envisaged that cariporide administration would also probably have reduced pulmonary artery remodeling. The failure to observe this may reflect a number of factors, including differences in stimuli to induce vascular hypertrophy or tissue-specific differences in NHE-1-dependent vascular responses. With respect to the latter, note that inhibition of smooth muscle cell proliferation by NHE-1 inhibitors has not been demonstrated in pulmonary arteries, thus raising the possibility that these vessels undergo remodeling through a NHE-1-independent pathway.

Our results therefore demonstrate that the effect of cariporide is restricted to direct inhibition of the compensatory myocardial responses to MCT-induced resultant pulmonary vascular remodeling. The beneficial effects were clearly observed with respect to a variety of indices, including reduced RV hypertrophy and complete abrogation of morphological abnormalities as well as improved function including attenuation of heart failure. The attenuation of RV hypertrophy was documented by using multifaceted approaches, including measurement of cell size, tissue gravimetric analysis, and determination of expression of ANP, which is known to be increased in the hypertrophied myocardium (Durocher et al., 1998). Moreover, NHE-1 RV mRNA expression was also elevated in response to MCT, albeit to a lesser degree than ANP, although this was prevented by cariporide. Although the results indicate an up-regulation of both genes, note that mRNA expression was done using semiquantitative approaches, which limits detailed interpretation of the data. Weight gain, which has been shown to be greatly reduced after MCT administration (Kodama and Adachi, 1999), was twice that in the cariporide group treated with MCT when compared with MCT alone, further demonstrating that animals on cariporide treatment fared better than their un-

treated counterparts, further suggesting a marked reduction in morbidity in these animals.

The precise mechanism for the salutary effect of cariporide on compensatory myocardial response needs to be determined especially in view of the latter's complex nature. For example, RV hypertrophy following MCT treatment is associated with increased oxidative stress (Pichardo et al., 1999), elevations in both  $\alpha_1$ - and  $\beta$ -adrenergic receptor densities (Chen et al., 1999), reduced natriuretic peptide receptors (Kim et al., 1999), up-regulation of the endothelin system (Ueno et al., 1999), electrophysiological changes (Lee et al., 1997), as well as the dispersion and disorganization of the principal gap junction protein connexin 43 (Uzzaman et al., 2000). Therefore, the RV hypertrophy following MCT treatment is undoubtedly a complex phenomenon. As referred to above, the role of NHE-1 probably lies in its ability to contribute to the hypertrophic process, but how this occurs is unknown. Recent evidence suggests that sodium ions may represent a key factor. In this regard, note that NHE-1 is a significant source of sodium entry into the cardiac cell and that sodium ions are known to be important mediators of cell hypertrophy (Gu et al., 1999; Hayasaki-Kajiwara et al., 1999). One hypothesis suggests that the role of sodium reflects its ability to activate distinct PKC isoforms, especially PKC $\delta$  and PKC $\epsilon$ , resulting in increased protein synthesis and hypertrophy (Hayasaki-Kajiwara et al., 1999). Other hypotheses have also been proposed, including the NHE-1-dependent activation of both Raf-1 and MAP kinase resulting in cardiomyocyte hypertrophy (Yamazaki et al., 1998). Further studies are necessary to identify the precise mechanism(s) underlying what appears to be a critical role for NHE-1 in RV hypertrophy as well as the antiporter's role in myocardial remodeling in general.

In conclusion, our study demonstrates that a NHE-1-selective inhibitor, cariporide, attenuates the RV hypertrophy and heart failure after MCT administration in rats in the absence of effect of pulmonary vessel remodeling. Taken together, the results suggest an antihypertrophic effect of the drug on the myocardium as well as a contributory role of NHE-1 in the myocardial adaptive response to pulmonary vascular injury in this model. Our results suggest that in principle, NHE-1 inhibition represents a desirable approach to reduce the RV involvement in pulmonary hypertension, particularly in conjunction with other therapies aimed at targeting the primary pulmonary artery dysfunction.

#### Acknowledgments

We thank Aventis Pharma (Frankfurt, Germany) for providing us with experimental diets and for performing analysis of serum cariporide levels.

#### References

Chen EP, Akhter SA, Bittner HB, Koch WJ, Davis RD and Van Trigt P (1999) Molecular and functional mechanisms of right ventricular adaptation in chronic pulmonary hypertension. *Ann Thorac Surg* **67**:1053–1058.  
 Cingolani HE (1999)  $\text{Na}^+/\text{H}^+$  exchange hyperactivity and myocardial hypertrophy: are they linked phenomena? *Cardiovasc Res* **44**:462–467.  
 Durocher D, Grepin C and Nemer M (1998) Regulation of gene expression in the endocrine heart. *Recent Prog Horm Res* **53**:7–23.

Gainé SP and Rubin LJ (1998) Primary pulmonary hypertension. *Lancet* **352**:719–725.  
 Gu JW, Anand V, Shek EW, Moore MC, Brady AL, Kelly WC and Adair TH (1999) Sodium induces hypertrophy of cultured myocardial myoblasts and vascular smooth muscle cells. *Hypertension* **31**:1083–1087.  
 Gumina RJ, Buerger E, Eickmeier C, Moore J, Daemngen J and Gross GJ (1999) Inhibition of the  $\text{Na}^+/\text{H}^+$  exchanger confers greater cardioprotection against 90 minutes of myocardial ischemia than ischemic preconditioning in dogs. *Circulation* **100**:2519–2516.  
 Gumina RJ and Gross GJ (1999) If ischemic preconditioning is the gold standard, has a platinum standard of cardioprotection arrived? Comparison with NHE inhibition. *J Thromb Thrombolysis* **8**:39–44.  
 Gundersen HJ, Jensen TB and Osterby R (1978) Distribution of membrane thickness was determined by linear analysis. *J Microsc* **113**:27–43.  
 Hayasaki-Kajiwara Y, Kitano Y, Iwasaki T, Shimamura T, Naya N, Iwaki K and Nakajima M (1999)  $\text{Na}^+$  influx via  $\text{Na}^+/\text{H}^+$  exchange activates protein kinase C isozymes  $\delta$  and  $\epsilon$  in cultured neonatal rat cardiac myocytes. *J Mol Cell Cardiol* **31**:1559–1572.  
 Hoque N, Cook MA and Karmazyn M (2000) Inhibition of  $\alpha_1$ -adrenergic-mediated responses in rat ventricular myocytes by adenosine  $\text{A}_1$  receptor activation: role of the  $\text{K}_{\text{ATP}}$  channel. *J Pharmacol Exp Ther* **294**:770–777.  
 Hori M, Nakatsubo N, Kagiya T, Iwai K, Sato H, Iwakura K, Kitabatake A and Kamada T (1990) The role of  $\text{Na}^+/\text{H}^+$  exchange in norepinephrine-induced protein synthesis in neonatal cultured cardiomyocytes. *Jpn Circ J* **54**:535–539.  
 Jandeleit-Dahm K, Hannan KM, Farrelly CA, Allen TJ, Rumble JR, Gilbert RE, Cooper ME and Little PJ (2000) Diabetes-induced vascular hypertrophy is accompanied by activation of  $\text{Na}^+/\text{H}^+$  exchange and prevented by  $\text{Na}^+/\text{H}^+$  exchange inhibition. *Circ Res* **87**:1133–1140.  
 Jensen EB, Gundersen HJ and Osterby R (1979) Determination of membrane thickness distribution from orthogonal intercepts. *J Microsc* **115**:19–33.  
 Karmazyn M, Gan XT, Humphreys RA, Yoshida H and Kusumoto K (1999) The myocardial  $\text{Na}^+/\text{H}^+$  exchange: structure, regulation, and its role in heart disease. *Circ Res* **85**:777–786.  
 Kim SZ, Cho KW and Kim SH (1999) Modulation of endocardial natriuretic peptide receptors in right ventricular hypertrophy. *Am J Physiol* **277**:H2280–H2289.  
 Kodama K and Adachi H (1999) Improvement of mortality by long-term E4010 treatment in monocrotaline-induced pulmonary hypertensive rats. *J Pharmacol Exp Ther* **290**:748–752.  
 Kranzhöfer R, Schirmer J, Schömig A, von Hodenberg E, Pestel E, Metz J, Lang HJ and Kübler W (1993) Suppression of neointimal thickening and smooth muscle cell proliferation after arterial injury in the rat by inhibitors of  $\text{Na}^+/\text{H}^+$  exchange. *Circ Res* **73**:264–268.  
 Krowka MJ (2000) Pulmonary hypertension: diagnostics and therapeutics. *Mayo Clin Proc* **75**:625–630.  
 Kusumoto K, Haist JV and Karmazyn M (2001)  $\text{Na}^+/\text{H}^+$  exchange inhibition reduces hypertrophy and heart failure after myocardial infarction in rats. *Am J Physiol* **280**:H738–H745.  
 Lee JK, Kodama I, Honjo H, Anno T, Kamiya K and Toyama J (1997) Stage-dependent changes in membrane currents in rats with monocrotaline-induced right ventricular hypertrophy. *Am J Physiol* **272**:H2833–H2842.  
 Lilienfeld DE and Rubin LJ (2000) Mortality from primary pulmonary hypertension in the United States, 1979–1996. *Chest* **117**:796–800.  
 Nakazawa H, Hori M, Ozaki H and Karaki H (1999) Mechanisms underlying the impairment of endothelium-dependent relaxation in the pulmonary artery of monocrotaline-induced pulmonary hypertensive rats. *Br J Pharmacol* **128**:1098–1104.  
 Pichardo J, Palace V, Farahmand F and Singal PK (1999) Myocardial oxidative stress changes during compensated right heart failure in rats. *Mol Cell Biochem* **196**:51–57.  
 Pierce GN and Czubyrt MP (1995) The contribution of ionic imbalance to ischemia/reperfusion-induced injury. *J Mol Cell Cardiol* **27**:53–63.  
 Rosenberg HC and Rabinovitch M (1998) Endothelial injury and vascular reactivity in monocrotaline pulmonary hypertension. *Am J Physiol* **255**:H1484–H1491.  
 Schultze AE and Roth RA (1998) Chronic pulmonary hypertension—the monocrotaline model and involvement of the hemostatic system. *J Toxicol Environ Health B Crit Rev* **1**:271–346.  
 Ueno M, Miyauchi T, Sakai S, Kobayashi T, Goto K and Yamaguchi I (1999) Effects of physiological or pathological pressure load in vivo on myocardial expression of ET-1 and receptors. *Am J Physiol* **277**:R1321–R1330.  
 Uzzaman M, Honjo H, Takagishi Y, Emdad L, Magee AI, Severs NJ and Kodama I (2000) Remodeling of gap junctional coupling in hypertrophied right ventricles of rats with monocrotaline-induced pulmonary hypertension. *Circ Res* **86**:871–878.  
 Yamazaki T, Komuro I, Kudoh S, Zou Y, Nagai R, Aikawa R, Uozumi H and Yazaki Y (1998) Role of ion channels and exchanger in mechanical stretch-induced cardiomyocyte hypertrophy. *Circ Res* **82**:430–437.  
 Yoshida H and Karmazyn M (2000)  $\text{Na}^+/\text{H}^+$  exchange inhibition attenuates hypertrophy and heart failure in 1-wk postinfarction rat myocardium. *Am J Physiol* **278**:H300–H304.

**Address correspondence to:** Dr. Morris Karmazyn, Department of Pharmacology and Toxicology, University of Western Ontario, Medical Sciences Building, London, Ontario N6A 5C1 Canada. E-mail: mkarm@uwo.ca